Remote Sensing of Environment 312 (2024) 114340

Contents lists available at ScienceDirect

Remote Sensing of Environment

journal homepage: www.elsevier.com/locate/rse

Intertidal seagrass extent from Sentinel-2 time-series show distinct trajectories in Western Europe

Bede Ffinian Rowe Davies [a,*], Simon Oiry [a], Philippe Rosa [a], Maria Laura Zoffoli [b], Ana I. Sousa [c], Oliver R. Thomas [d], Dan A. Smale [e], Melanie C. Austen [d], Lauren Biermann [d], Martin J. Attrill [d,i], Alejandro Roman [f], Gabriel Navarro [f], Anne-Laure Barillé [g], Nicolas Harin [g], Daniel Clewley [h], Victor Martinez-Vicente [h], Pierre Gernez [a], Laurent Barillé [a]

[a] Nantes Université, Institut des Substances et Organismes de la Mer, ISOMer, UR2160, Nantes F-44000, France
[b] Consiglio Nazionale delle Riecerche, Instituto di Science Marine (CNR-ISMAR), Rome, Italy
[c] ECOMARE–Laboratory for Innovation and Sustainability of Marine Biological Resources, CESAM–Centre for Environmental and Marine Studies, Department of Biology, University of Aveiro, Campus Universitário de Santiago, Aveiro, Portugal
[d] School of Biological and Marine Science, University of Plymouth, Plymouth PL4 8AA, United Kingdom
[e] Marine Biological Association of the UK, Citadel Hill, Plymouth PL1 2PB, UK
[f] Institute of Marine Sciences of Andalusia (ICMAN-CSIC), Spanish National Research Council (CSIC), Department of Ecology and Coastal Management; 11510 Puerto Real, Spain
[g] Bio-littoral, Immeuble Le Nevada, 2 Rue du Château de l'Eraudière, 44300 Nantes, France
[h] Plymouth Marine Laboratory, Prospect Place, The Hoe, Plymouth, UK
[i] Ocean Conservation Trust, Rope Walk, Coxside, Plymouth, PL4 0LF, UK

ARTICLE INFO

Editor: Menghua Wang

Keywords:
Intertidal seagrass
Habitat monitoring
Trajectory analysis
Neural network
Bayesian general additive model

ABSTRACT

Intertidal areas, which emerge during low tide, form a vital link between terrestrial and marine environments. Seagrasses, a well-studied intertidal habitat, provide a multitude of different ecosystem goods and services. However, owing to their relatively high exposure to anthropogenic impacts, seagrasss meadows and other intertidal habitats have seen extensive declines. Remote sensing methods that can capture the spatial and temporal variation of marine habitats are essential to best assess the trajectories of seagrass ecosystems. An advanced machine learning method has been developed to map intertidal vegetation from satellite-derived surface reflectance at a 12-band multispectral resolution and distinguish between similarly pigmented intertidal macrophytes, such as seagrass and green algae. The Intertidal Classification of Europe: Categorising Reflectance of Emerged Areas of Marine vegetation with Sentinel-2 (ICE CREAMS v1.0), a neural network model trained on over 300,000 Sentinel-2 pixels to identify different intertidal habitats, was applied to the open-access long term archive of systematically collected Sentinel-2 imagery to provide 7 years (2017–2023) worth of intertidal seagrass dynamics in 6 sites across Western Europe (471 Sentinel-2 Images). A combination of independently collected visually inspected Uncrewed Aerial Vehicle imagery and in situ quadrat images were used to validate ICE CREAMS. Having achieved a high seagrass classification accuracy (0.82 over 12,000 pixels) and consistent conversion into cover (19% RMSD), the ICE CREAMS model outputs provided evidence of site specific variation in trajectories of seagrass extent, when appropriate consideration of intra-annual variation has been considered. Inter-annual dynamics of sites showed some instances of consistent change, some indicated stability, while others indicated instability over time, characterised by increases and decreases across the time-series in seagrass coverage. This methological pipeline has helped to create up-to-date monitoring data that, with the planned continuation of the Sentinel missions, will allow almost real-time monitoring of these habitats into the future. This process, and the data it provides, could aid management practitioners from regional to international levels, with the ability to monitor intertidal seagrass meadows at both high spatial and temporal resolution, over continental scales. The implementation of Earth Observation for high-resolution monitoring of intertidal seagrasses could therefore allow for gap-filling seagrass datasets, and sustain specific and rapid management measures.

* Corresponding author.
E-mail address: bede.davies@univ-nantes.fr (B.F.R. Davies).

https://doi.org/10.1016/j.rse.2024.114340
Received 5 April 2024; Received in revised form 22 July 2024; Accepted 26 July 2024
Available online 3 August 2024

1. Introduction

1.1. Seagrass

Seagrasses, the only group of truly marine flowering plants, form extensive meadows around coastal and intertidal areas across the majority of the globe. Through provisioning of many socio-economic and ecological benefits, seagrasses are highly valued marine ecosystems (e.g. climate regulation through carbon sequestration, coastal stabilisation, habitat provisioning, water quality mediation, fisheries production: Devoy, 2008; Hillebrand et al., 2018; Jackson et al., 2015; Lamb et al., 2017; Paul and Amos, 2011; Sousa et al., 2019; Unsworth et al., 2019; Zoffoli et al., 2022). Yet, these habitats, which are sensitive to human disturbance, eutrophication, marine heat waves and ocean acidification, have been shown to be globally threatened (Losciale et al., 2024). This led to the European Union (EU) including seagrasses within the Water Framework Directive (WFD) as a *biological quality element* alongside phytoplankton, macroalgae, benthic invertebrate fauna and fish (Foden and Brazier, 2007; Krause-Jensen et al., 2005), with member states needing to make sure these *biological quality elements* are in 'good ecological status'. The WFD requirements have increased efforts to monitor, conserve and restore coastal habitats and species. To establish a baseline of reference for setting a 'good ecological status', historic data were used with best available contemporary data as a comparison. This type of trend analysis is often fraught with data availability issues with consistency, repetition of sampling and comparability of methods increasing uncertainty, as well as inter-comparison of habitat ecological status between regions.

1.2. Trends in seagrass

Many studies have aimed at assessing or estimating trends in seagrasses at global or continental scales, seeking to catalogue historic literature records of seagrass and using historic data to assess trends in the available time-series (Dunic et al., 2021; Los Santos et al., 2019; McKenzie et al., 2020). However, temporal assessments come up against many inherent practical issues or biases associated with the scales and resolutions of the data available: spatial, temporal, bioregional, taxonomic and ecological. Los Santos et al. (2019) assessed taxonomically explicit data across Europe from 1986 to 2016, yet reported lacking temporal regularity, especially before 1950. Alternatively, in a global assessment, McKenzie et al. (2020) found limitations in the distribution of data across bioregions, with vast areas of the globe with no or limited observations. Dunic et al. (2021), updating previously catalogued data (Waycott et al., 2009), assessed trends by bioregions, but also highlighted biases in these historic data, such as selection bias where easy to access sites are more studied, or sites that showed stable meadows were not published. While taxonomic consistencies are not common across continental spatial scales, with different species occupying similar habitats across ecoregions, distinct divisions in ecology of seagrasses can be seen globally, the most obvious of which is the split between intertidal and subtidal seagrasses. Yet, none of the above studies have taken the inherent differences, such as their resilience to regular aerial exposure and desiccation that requires high levels of temperature plasticity, between these two ecological subsets of seagrasses into account. While some of the issues, such as availability of historic data, are impossible to remedy, others, such as temporal consistency, bioregional bias and ecological distinctions, can be addressed by combining historic data and local knowledge with novel techniques for seagrass monitoring.

1.3. Remote sensing

Through the use of Remote Sensing (RS) in the form of Uncrewed Aerial Vehicle (UAV) and satellite derived Earth Observation (EO) imagery, issues relating to temporal, regional and spatial consistency can be suitably addressed. Satellite RS imagery utilises multi- or hyperspectral imagery to observe specific phenomena and can cover vast areas (global), provide consistent repeat measurements (days) and/or return high spatial resolution imagery (30 cm). However, increases in spatial, temporal or spectral resolution is often balanced by decreases in the other factors (Veettil et al., 2020). Satellite RS has been used at the global scale to map trends in terrestrial habitats, such as crops, rain forest or desert extent (Caparros-Santiago et al., 2021; Guan et al., 2014; Rankine et al., 2017; Zhong et al., 2016). In coastal and open oceans, Satellite RS has been used to study habitats and natural phenomena, such as subtidal seagrasses, phytoplankton blooms or floating macroalgae (Dai et al., 2023; Dierssen et al., 2015; Gernez et al., 2023; Kutser et al., 2020; Lee et al., 2023; Traganos et al., 2022; Traganos and Reinartz, 2018). Intertidal areas have rarely been assessed globally using RS, yet some notable examples exist, where authors have leveraged state-of-the-art machine learning alongside geo-spatial techniques to map intertidal habitats, such as saltmarsh, tidal flats, kelp and mangrove forests (Campbell et al., 2022; Jia et al., 2023; Mora-Soto et al., 2020; Murray et al., 2019). On smaller scales monospecific intertidal seagrass meadows have been assessed with RS (Zoffoli et al., 2022; Zoffoli et al., 2020), yet some issues have been highlighted with using multispectral imagery to distinguish between similarly pigmented green macroalgae and seagrasses in mixed assemblages (Phinn et al., 2018; Veettil et al., 2020), thus challenging large-scale assessments.

1.4. Neural networking with RS

As the observational methods have developed so have the methods used to analyse them. Machine learning techniques for regression or classification have become commonplace in remote sensing tasks with many open access data products being the output of machine learning methods, such as terrestrial land use, global surface temperature, weather forecasting, urban mapping, oceanic chlorophyl concentration, water depth in shallow seas, surface and subsurface marine temperature, and oil spill prediction (Ai et al., 2020; Hoang and Tran, 2021; Li et al., 2020; Shamsudeen, 2020; Su et al., 2021; Vilas et al., 2011). These machine learning methods allow, and are even improved by having, large numbers of model parameters, regardless of collinearity. Therefore, classification predictions are able to utilise all bands of multispectral data to improve predictive capability. Using a comprehensive in situ spectral library, a previous study demonstrated that machine learning algorithms can discriminate soft-bottom intertidal vegetation classes at high accuracy from reflectance measurements; in particular, we showed that a multispectral sensor with at least 8 spectral bands in the visible and near-infrared spectral ranges had the potential to separate seagrass from red, brown and green macroalgae (Davies et al., 2023a). Building on such promising results, the objective of the present work was to upscale the approach to satellite imagery across several intertidal seagrass sites in Europe.

1.5. Summary of approach

Here we built a machine learning neural network to predict intertidal seagrass habitat from 10 m resolution Sentinel-2 imagery to assess recent trajectories (2017–2023) in intertidal seagrass extent across six sites in Western Europe, some of which have previously been assessed for long-term trends (Los Santos et al., 2019). Using the 7 years of long-term archive satellite imagery, made publicly available on the Copernicus database, we display an almost real-time method for assessing intertidal seagrass extent observed during low tide (i.e. emerged seagrass), update the current trajectories of these sites in relation to previous publications and highlight how the relatively low spectral resolution Sentinel-2 satellite mission, alongside modern machine

learning techniques, can distinguish mixed intertidal habitats with high levels of accuracy over large spatial and geographical ranges.

2. Materials and methods

2.1. General methodological workflow

To create data that would allow a high resolution analysis of recent trends in intertidal seagrass cover, a workflow with three main steps was created (Fig. 1). Temporally and spatially explicit UAV-derived habitat data were assigned to concurrent Sentinel-2 multispectral bottom-of-atmosphere (BOA) reflectance, standardised reflectance (Eq. 1), Normalised Difference Vegetation Index (NDVI: Eq. 2) and Normalised Difference Water Index (NDWI: Eq. 3), which was then used to train and build a neural network classification model to identify intertidal habitats from Sentinel-2 imagery, with independent auxiliary in situ data used to validate. Finally, each pixel classified as seagrass was converted to seagrass cover (%: Eq. 4) derived from its NDVI.

3. Neural network intertidal classifier

3.1. Training data

3.1.1. Habitat labelling

Training data were collated across a range of methods. The vast majority of the training dataset was collected through the use of a multispectral UAV to provide both geographically and temporally explicit delineation of known intertidal habitats. All UAV flights were performed during low tide and during favourable (low cloud cover) atmospheric conditions, meaning that the intertidal habitats were observed during emersion. The UAV-derived habitat data mostly covered vegetated soft-bottom intertidal areas and seagrass was identified from aerial imagery using visual inspection, as the high spatial resolution of pixels (from 8 mm to 80 mm) allowed for accurate identification. From the high resolution UAV imagery, resampled 10 m macro-pixels, characterised by the dominant habitat class (modal class), were used to train the Sentinel-2 classifier. Then, Sentinel-2 pixels of

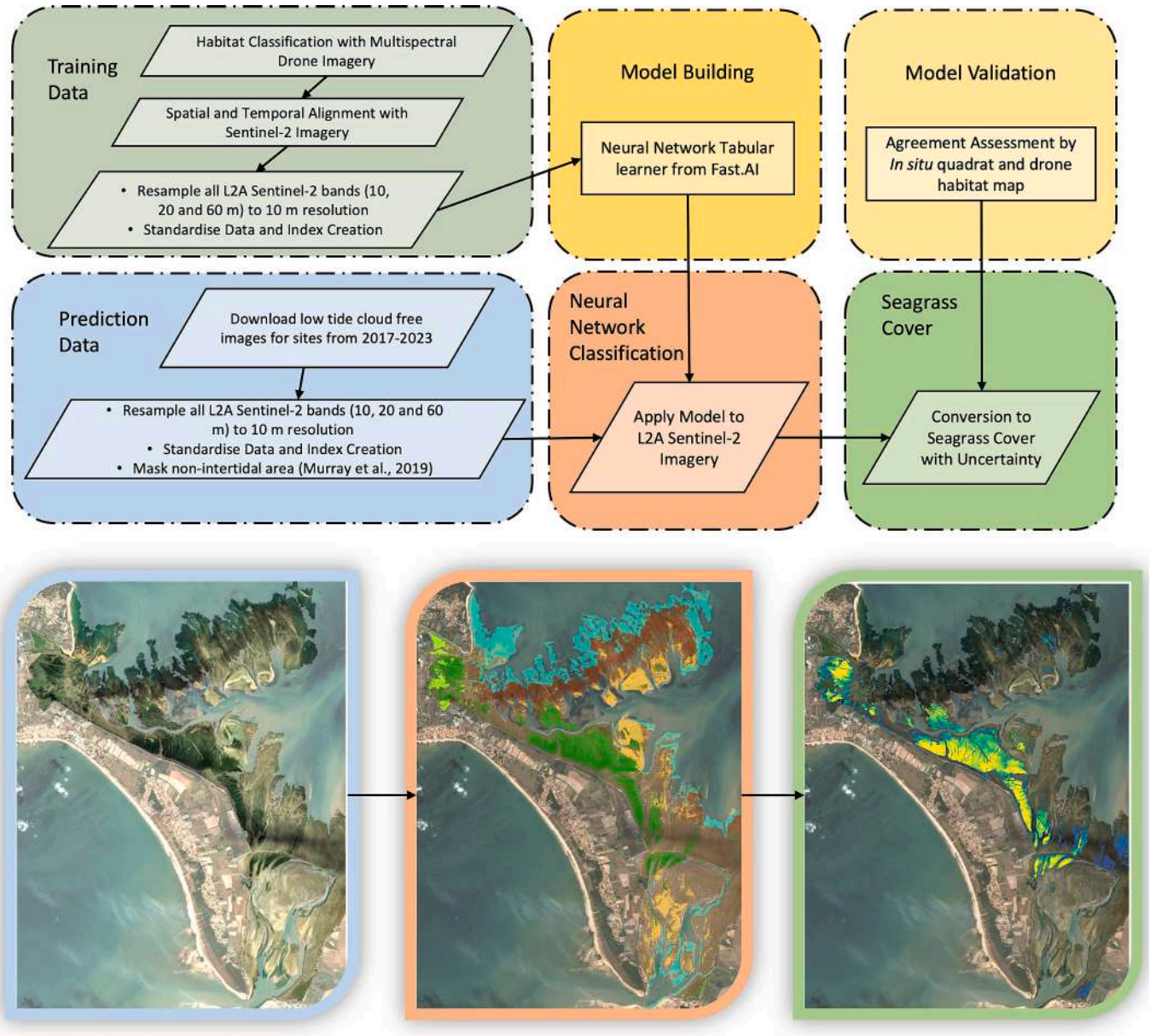

Fig. 1. Workflow showing process for neural network classification model building and seagrass cover (%) from this classification, with example images showing process from Sentinel-2 Data to Habitat Classification to Seagrass Cover (%).

some classes such as bare sediments (mud and sand), sediments containing high abundances of microphytobenthos, as well as hard substrates covered by vegetation, were added to the training dataset to increase the balance between classes (i.e. Bay of Veys, Jersey, Penzé and Aiguillon Bay: Fig. 2). These additional pixels were selected through visual inspection of Sentinel-2 imagery.

3.1.2. Alignment with Sentinel-2 imagery

Geolocated Level-2 A (L2A) Sentinel-2 A/B images that coincided spatially and temporally (+/− 15 days) with these UAV acquisitions were downloaded from the European Space Agency (ESA) data portal. L2A data have already been atmospherically corrected using the Sen2-Cor processing algorithm (Main-Knorn et al., 2017), and are distributed as BOA reflectance. Visual inspection was used to select cloud free and low tide Sentinel-2 images. To avoid the effect of submerged pixels being misclassified, a class of water pixels was also included within the model. All 12 bands of Sentinel-2 were resampled to 10 m resolution (20 and 60 m band values being repeated 4 and 36 times), labelled and standardised following a Min-Max Standardisation (Davies et al., 2023a; Douay et al., 2022).

$$R_i^*(\lambda) = \frac{R_i(\lambda) - min(R_i)}{max(R_i) - min(R_i)} \quad (1)$$

where $R_i(\lambda)$ is the BOA reflectance at a specific band (λ) for a specific pixel (i), where min(R_i) and max(R_i) are the corresponding minimum and maximum values across the bands for that pixel. Furthermore, NDVI and NDWI were calculated for each pixel from the BOA Sentinel-2 reflectance values:

$$NDVI = \frac{R(832) - R(664)}{R(832) + R(664)} \quad (2)$$

$$NDWI = \frac{R(560) - R(832)}{R(560) + R(832)} \quad (3)$$

with $R(560)$, $R(664)$ and $R(832)$ being the green (Sentinel-2 band centred on 560 nm), red (Sentinel-2 band centred on 664 nm) and near-infrared (Sentinel-2 band centred on 832 nm) spectral domains respectively.

Pixels were labelled into 9 classes: Bare Sand, Bare Mud, Ulvophyceae (green macroalgae), Magnoliopsida (seagrass), Microphytobenthos (unicellular photosyntheic eukaryotes and cyanobacteria), Mixed-Rocks and Phaeophyceae (brown macroalgae), Rhodophyceae (red macroalgae), Xanthophyceae (yellow-green macroalgae) and Water. Within the Magnoliopsida class, there is a maximum diversity of three species (*Nanozostera noltei*, *Zostera marina* and *Cymodocea nodosa*), although *Nanozostera noltei* was the dominant species across most intertidal sites assessed.

3.1.3. Model building

373,814 labelled pixels consisting of 26 features (12 BOA reflectances, 12 standardised reflectances, NDVI and NDWI), were used to train a deep learning, neural network, tabular learner from the FastAI framework in Python v3 (Howard and Gugger, 2020; Van Rossum and Drake, 2009). The model consisted of 2 hidden layers with 26,761 trainable parameters and was fine-tuned across 20 epochs to minimise cross entropy loss using the ADAptive Moment estimation (ADAM) optimiser. The final within-sample error rate was 0.0365. The model, named the Intertidal Classification of Europe: Categorising Reflectance of Emerged Areas of Marine vegetation with Sentinel-2 (ICE CREAMS v1.0), provided a classification for each pixel, based on the greatest probability class. For every pixel where seagrass was predicted, the Seagrass Cover (SC: %) was calculated as in Zoffoli et al. (2020):

$$SC = 172.06 * NDVI - 22.18 \quad (4)$$

Following this method only SC values above 20% were selected.

3.1.4. Validation data

To ensure validation of the ICE CREAMS model was independent of model building, several methods were employed to generate validation data. Field campaigns were carried out by taking geo-located photo quadrats (Davies et al., 2023b). In situ photo quadrats were taken within the Tagus Estuary and Ria de Aveiro Coastal Lagoon (Portugal), as well as in Bourgneuf Bay (France). Further validation data were collected through Red Green Blue (RGB) UAV imagery, taken within two estuaries in the UK (Tamar and Kingsbridge) and a bay in Spain (Cádiz) as well as in situ samples collected within Ria D'Etel in France (Fig. 2). Global

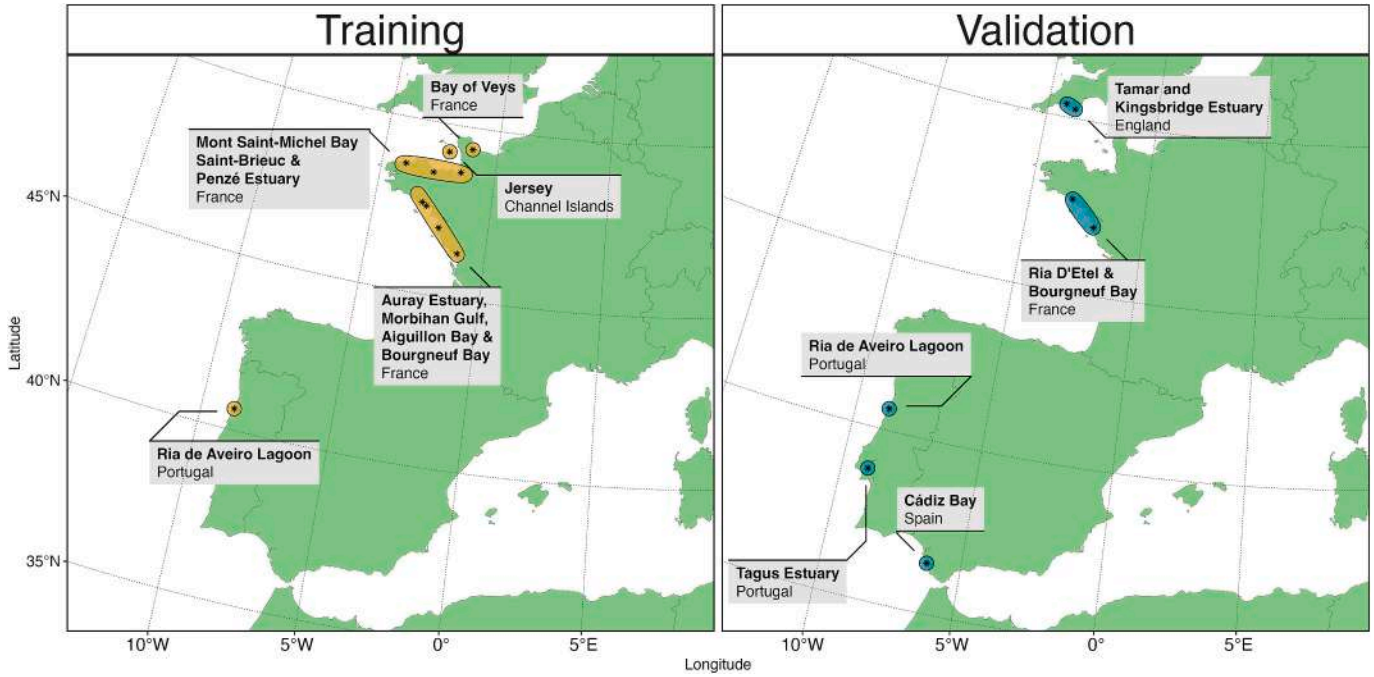

Fig. 2. Training and Validation data collection sites across Europe.

accuracy (G_a: Eq. 5), specificity (G_{spe}: Eq. 6) and sensitivity (G_{sen}: Eq. 7) of the ICE CREAMS model were calculated across all validation data as binary presence (positive) or absence (negative) of seagrass across ~12,000 Sentinel-2 pixels: ~5000 Seagrass Pixels and ~ 7000 Non-Seagrass Pixels. Non-Seagrass pixels contained a range of the non-seagrass classes with ~1000 green macroalgae, ~3000 bare sand and mud, ~2000 microphytobenthos and ~ 1000 Mixed-Rocks with associated brown macroalgae.

$$G_a = \frac{TP + TN}{TP + TN + FP + FN} \tag{5}$$

$$G_{spe} = \frac{TN}{TN + FP} \tag{6}$$

$$G_{sen} = \frac{TP}{TP + FN} \tag{7}$$

for the number of Sentinel-2 satellite pixels categorised as true positive (*TP*), true negative (*TN*), false positive (*FP*) and false negative (*FN*). To assess agreement of NDVI-derived seagrass cover (SC_{NDVI}: %), Root Mean Squared Difference (*RMSD*: Eq. 8) was calculated comparing all quadrat-derived seagrass cover, taken from in situ field work ($SC_{Quadrat}$: %):

$$RMSD = \sqrt{\frac{1}{n}\Sigma_{i=1}^{n}\left(\frac{SC_{Quadrat_i} - SC_{NDVI_i}}{\sigma_i}\right)^2} \tag{8}$$

3.2. Trend assessment

3.2.1. Sites selected for intertidal seagrass extent assessment

Six sites were selected along the Western Atlantic Coast of Europe (Fig. 3). Sites were selected where known intertidal seagrass meadows were present and consistent imagery was available across the Sentinel-2 time series, unlike the training and validation data these sites could be

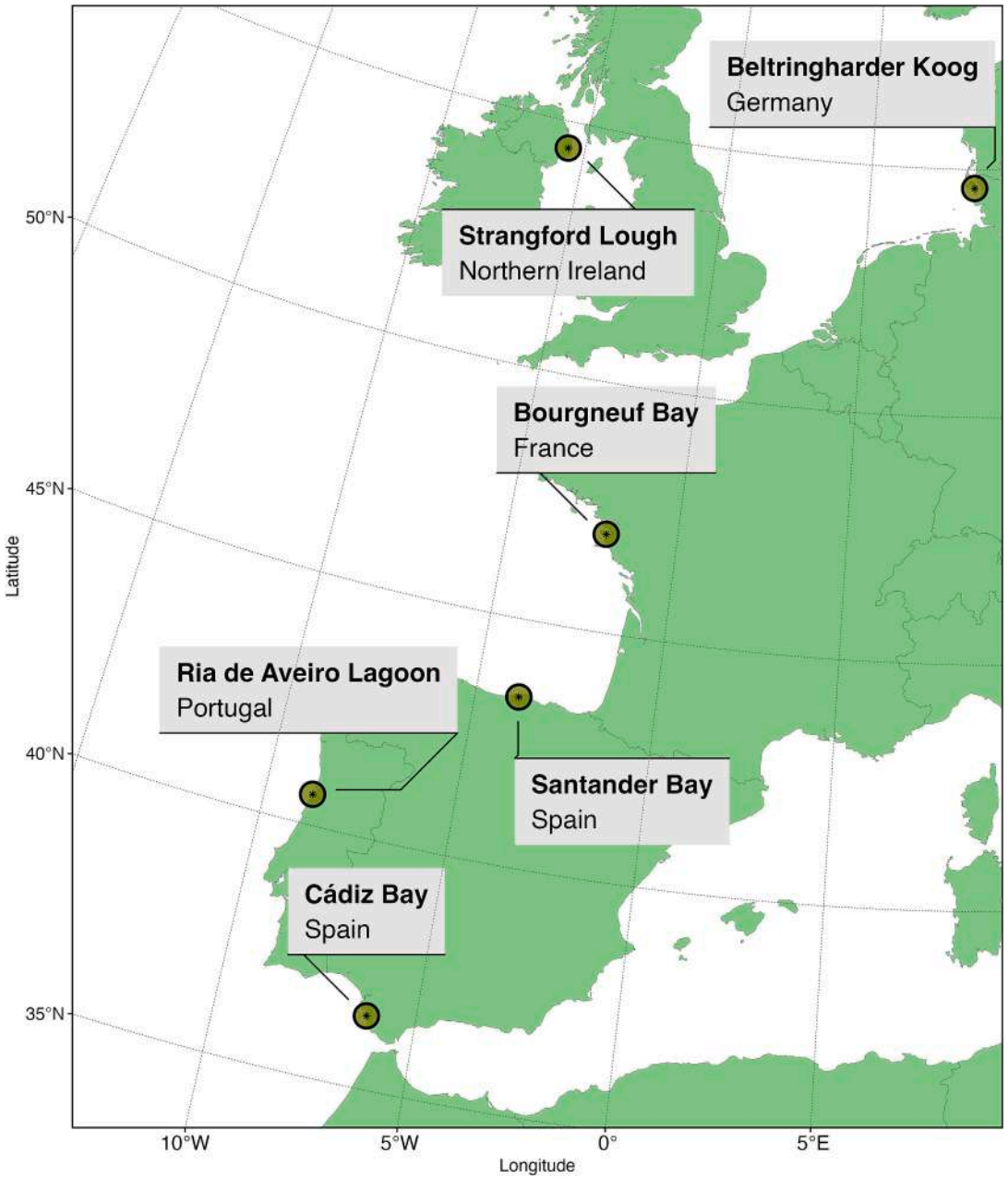

Fig. 3. Sites selected to analyse the interannual variability of intertidal seagrass across the North-East Atlantic.

situated in less accessible areas. For each site, all cloud free, low tide Sentinel-2 L2A images were selected from the Sentinel-2 Long Term Archive (LTA: Davies et al., 2024). A mask was used to isolate only pixels within the intertidal area (Murray et al., 2019). The ICE CREAMS Neural Network model was applied to classify intertidal habitats, and SC was computed within each seagrass pixel. As each pixel is 100 m^2 the summed SC within each site could be considered the total area covered by seagrass in m^2 per image. The uncertainty for each image (τ: Eq. 9) was calculated as the inverse of the mean of the per pixel probabilities from the ICES CREAMS model divided by the global accuracy when applied to validation data (G_a):

$$\tau = \frac{1-\overline{p}}{G_a} \tag{9}$$

3.2.2. Statistical analysis

A General Additive Model (GAM) (Wood, 2017) was used to assess trends of seagrass extent from all available seagrass extent maps across our sites; model parameters were estimated within a bayesian framework using the 'brms' and 'RStan' packages in R to leverage the Stan language (Bürkner, 2021; Carpenter et al., 2017; R Core Team, 2023; Stan Development Team, 2018). Observed total seagrass cover (E^*_i) and its uncertainty (τ_i) were modelled (Eq. 10) as a function of Time with a basis spline ($f(t_i)$) across Locations (ρ) and Day of the Year with a cyclic basis spline ($f(DOY_i)$) across Locations (ρ). The response variable was modelled assuming a Student-t distribution, with weakly informative priors (Student-T(3,0,2.5)). Model parameters were estimated using Markov Chain Monte Carlo (MCMC) sampling, with 4 chains of 5000 iterations and a warm-up of 200.

$$\begin{aligned} E^*_i &\sim Student(E_i, \tau_i) \\ E_i &\sim Student(\mu_i, \sigma_i) \\ \mu_i &= f(DOY_i) : \rho + f(t_i) : \rho \\ f(DOY_i) : \rho &\sim Student(3, 0, 2.5) \\ f(t_i) : \rho &\sim Student(3, 0, 2.5) \\ \sigma_i &\sim Student(3, 0, 2.5) \end{aligned} \tag{10}$$

3.2.3. Trend metrics

Rate of change in seagrass extent was taken as the first derivative of the model, using a sliding window of 365 days and reported as km^2 per year ($km^2\ y^{-1}$).

4. Results

4.1. Agreement assessment of ICE CREAMS model

Global accuracy of the ICE CREAMS model v1.0 across ~12,000 Sentinel-2 pixels was 0.815 showing a high confidence in the ability of the model to predict seagrass. Around 7000 of the validation pixels were non-seagrass, while around 5000 were seagrass, showing the agreement is based fairly evenly across both true-positives and true-negatives (Fig. 4 a). The model achieved a total sensitivity of 0.864 and a specificity of 0.742. Comparison of quadrat-derived with NDVI-derived seagrass cover (%) showed high agreement across quadrats, but with a small underestimation of NDVI-derived cover compared to quadrat compared cover (RMSD: 19%; Fig. 4 b).

4.2. Interannual trends

In all sites assessed, seagrass beds occupied areas of at least 2 km^2 at their maximum cumulative extent (Fig. 5). However, the distribution within the meadows was not consistent, with some beds showing large areas of relatively sparse seagrass cover (e.g. Strangford Lough), while others showed smaller areas of dense seagrass cover (e.g. Bourgneuf Bay), resulting in similar maximum cumulative extents (Fig. 5). Across some of the sites we can see consistent patterns of increase in intertidal seagrass extent from 2018 to late 2023, such as Santander and Cádiz Bay, while others, such as Ria de Aveiro Coastal Lagoon, showed a higher inter-annual variability in its maximum extent, with an initial decrease in 2019–2020 followed by an increase to initial levels (Fig. 6). No apparent change in intertidal seagrass was seen for Strangford Lough

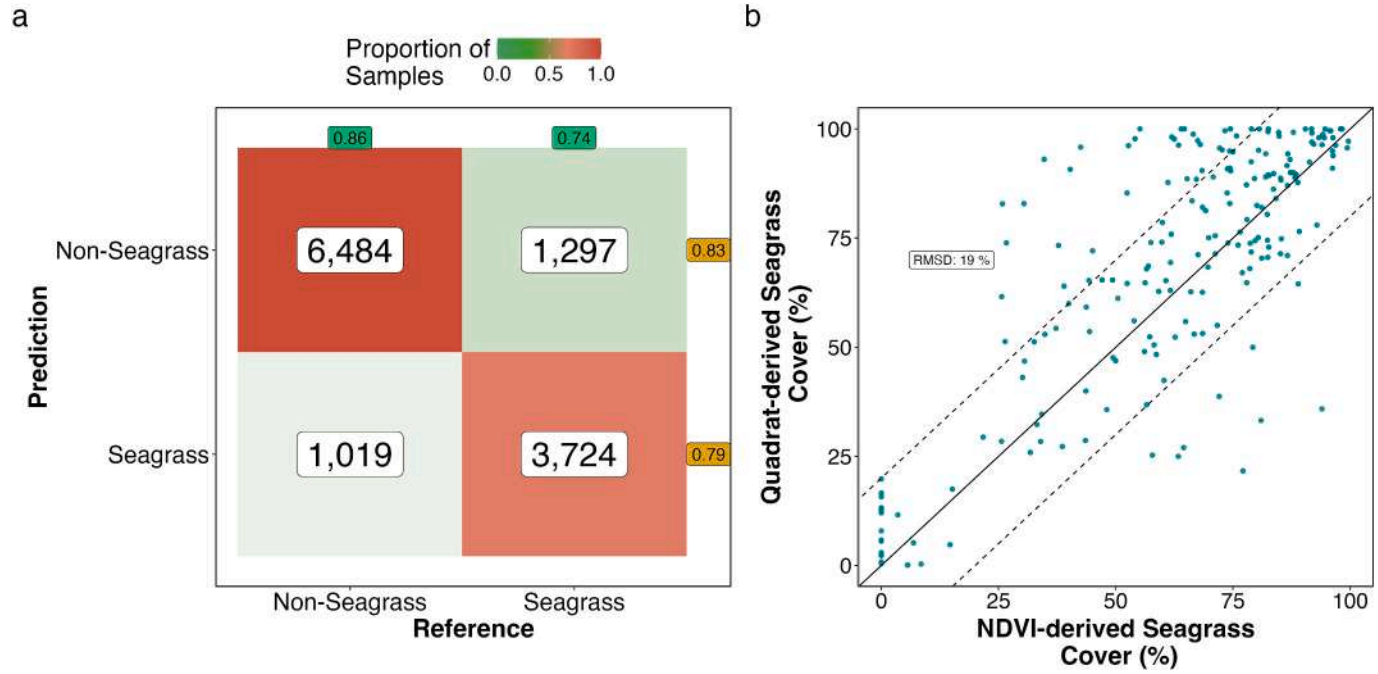

Fig. 4. Binary Validation of ICE CREAMS Neural Network model (a) and Comparison of in situ quadrat-derived with Sentinel-2 NDVI-derived seagrass cover (%) (b). Solid and dashed lines show 1:1 relationship with ±20% ranges. Confusion Matrix (a) shows proportion of Total Samples in agreement between Truth and Predicted Seagrass and Non-Seagrass pixels, with number of total pixels within each grid cell. External labels with numbers show within-class sensitivity and specificity in green and the Positive Predicted Value (PPV) and Negative Predicted Value (NPV) in gold. (For interpretation of the references to colour in this figure legend, the reader is referred to the web version of this article.)

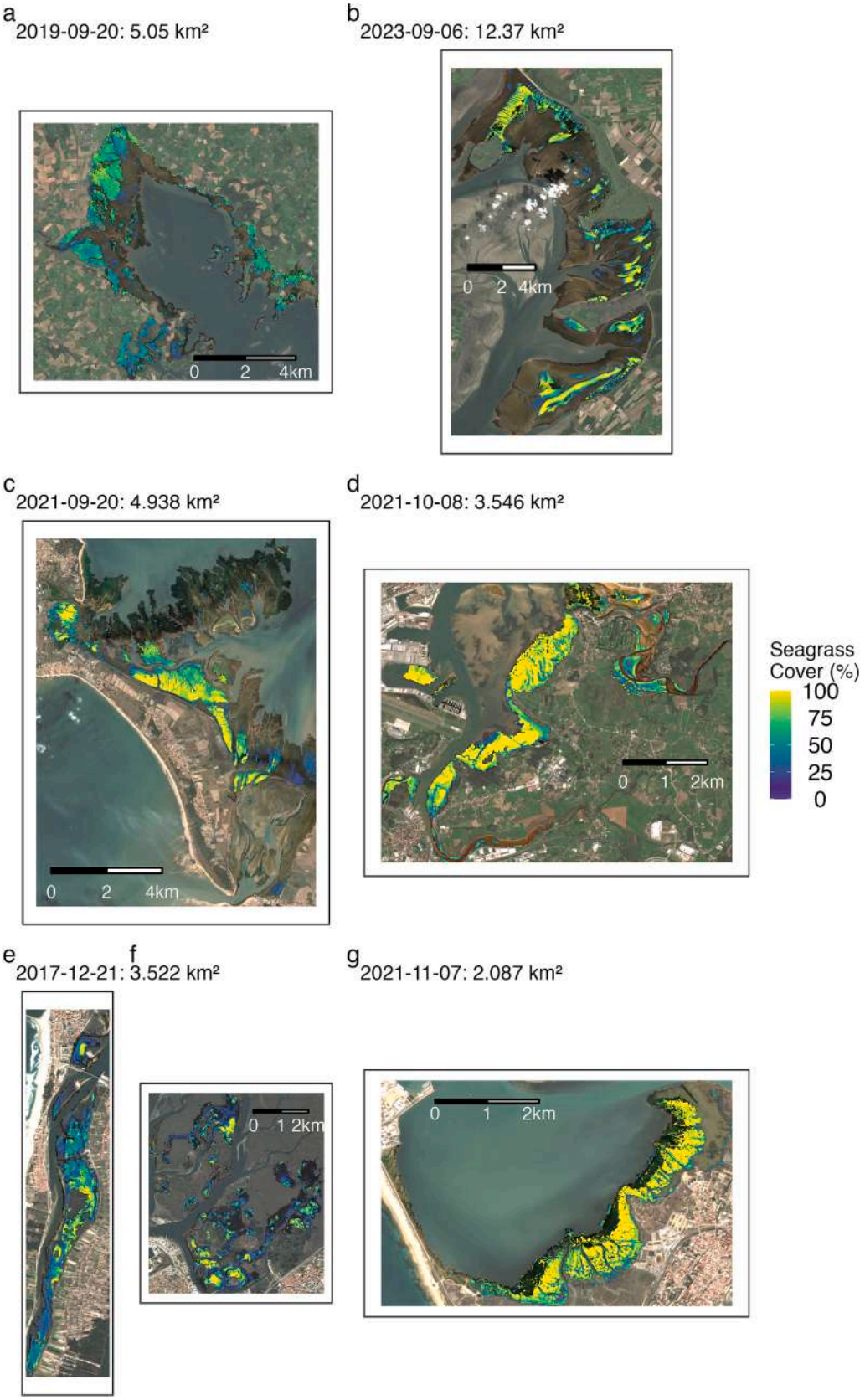

Fig. 5. Maximum Seagrass Cover images shown for all sites going from the north to the south Strangford Lough (a), Beltringharder Koog (b), Bourgneuf Bay (c), Santander Bay (d), Ria de Aveiro Coastal Lagoon (e & f) and Cádiz Bay (g).

or Beltringharder Koog. While Bourgneuf Bay consistently showed a seasonal decrease to a near-zero extent each winter until 2021 and 2022, Cádiz and Santander showed increases in the minimum yearly extent, as well as an increase in their maximum extent from the beginning of the time series. Modelled cumulative extent for the three increasing sites (Bourgneuf, Santander and Cádiz bay) showed percentage increases in the yearly maximums of 25%, 30% and 23.1%, respectively, between their peaks in 2018 and 2023. Relatively small peaks were seen in between yearly maxima in the two most northern sites Strangford Lough or Beltringharder Koog. Yet, these occurred during winter when the number of useable cloud free images were lower, which is indicated by the modelled uncertainty that is larger than the apparent peak, making any conclusions on the origin of this pattern problematic and requiring further investigation.

In terms of rate of change, the six sites showed distinct trajectories (Fig. 7), with Strangford Lough and Beltringharder Koog showing stable meadows surfaces across the time series. Significant rates of change in cumulative intertidal seagrass extent were observed for the other sites. Bourgneuf and Santander showed similar patterns, with consistent increases from 2020 to late 2021 and mid 2019 to mid 2021 respectively. Ria de Aveiro showed a significant decrease from 2018 to 2019 while a significant increase from 2019 to 2021. Cádiz bay showed significant growth for two periods, 2018 to 2019 and 2020 to 2021. Both Santander and Cádiz bay showed significant but small decreases in mid 2022.

4.3. Timing of maximal extent

There were differences in peak timing of maximum intertidal seagrass extent for all the sites (Fig. 8), from no changes in northern sites to variations across time in the most southern sites, ranging by up to 2 weeks. There are two clear groupings, with the most southern sites having peaks from mid/late October until late November. Further northern sites peaked in extent from late August to mid September. The earliest timing of maximal seagrass extent was seen in Beltringharder Koog, followed by Bourgneuf Bay then Strangford lough. Santander Bay showed the earliest maximum of the southern sites, followed by Cádiz Bay and Ria de Aveiro.

5. Discussion

Using an up-to-date time-series of Sentinel-2 imagery and a state of the art neural network algorithm (ICE CREAMS v1.0) we were able to assess inter-annual variation in intertidal seagrass extent across 6 sites in Western Europe. This algorithm and its conversion to seagrass cover allowed high confidence in the outputs (Fig. 4). Across the 7 years assessed (2017–2023), some sites showed increases in extent (e.g. Bourgneuf, Santander and Cádiz Bays), some sites showed consistency over time (e.g. Strangford Lough and Beltringhard Koog) and others (e.g. Ria de Aveiro Coastal Lagoon) showed early decreases followed by steady increase over time (Fig. 6). Generally, the sites further north showed consistency in extent and timing of maximum extent, while sites further south tended to show higher variation in extent and timing of maximum extent (Fig. 7 & Fig. 8). Timings of maximums were relatively consistent within the northern sites, while more southerly sites showed interannual variations.

5.1. A neural network classifier

One of the main barriers of RS for mapping intertidal habitats has been the heterogeneous nature of intertidal habitats, both spatially and temporally, but also in terms of biodiversity. Monospecific intertidal seagrass meadows have been mapped effectively using vegetation indices such as NDVI (Barillé et al., 2010; Lizcano-Sandoval et al., 2022; Zoffoli et al., 2022; Zoffoli et al., 2021; Zoffoli et al., 2020). However, when seagrasses are mixed with other intertidal macrophytes this approach is ineffective. The main challenge being the discrimination between seagrasses and green macroalgae sharing the same pigmentary composition (Oiry and Barillé, 2021; Phinn et al., 2018). This potential confusion has decreased the accuracy of seagrass mapping (Veettil et al., 2020). Using a spectral library, Davies et al. (2023a) showed that machine learning could help discriminate green macrophytes at the multispectral resolution of Sentinel-2. The current study demonstrated that this remains true when applied to Sentinel-2 images. This highlighted that advanced algorithms are needed to classify accurately and effectively soft-bottom intertidal habitats, as these habitats exhibit high spatial and temporal variability. As discussed, the Intertidal Classification of Europe: Categorising Reflectance of Emerged Areas of Marine vegetation with Sentinel-2 (ICE CREAMS) model, used here, was highly accurate for identifying seagrass pixels in relation to other vegetated and non-vegetated classes (Fig. 4). The ICE CREAMS model required a large quantity of training pixels (~375,000) to build a classifier that could achieve such accuracy across the 9 categories. These data covered 37.5 km^2 combining BOA and standardised reflectances alongside vegetation and water indices, the vast majority of which was provided by the use of multispectral UAV imagery from across the Atlantic coastline of Europe. The quantity and coverage of these data could not have been accomplished by in situ methods alone. Likewise, independent validation data (~ 12,000 pixels: 1.2 km^2) also relied upon multispectral UAV imagery from different areas of Europe than the training data. The importance of independence of validation is greatly emphasised for machine learning approaches (Maxwell et al., 2018; Murray et al., 2019); the agreement achieved from these independent data provides further proof of the applicability of the ICE CREAMS model when applied across Europe.

5.2. Technical limitations

While EO has many advantages over traditional in situ measurements, especially when trying to map large or inaccessible areas, there are also trade-offs to be considered. EO can cover vast areas, yet relies upon cloud free, and for intertidal assessments, low tide imagery. Furthermore, EO often has a balance of spectral, spatial and temporal resolution, with hyperspectral sensors providing lower spatial and temporal resolution (e.g. PRISMA: 240 spectral bands, 30 m spatial resolution and 7 days with off-nadir view but image acquisition depending on tasking request), and multi or lower spectral sensors providing higher spatial and temporal resolution (e.g. Sentinel-2: 10 Bands, 10 m spatial resolution and < 5 days, systematic worldwide cover of inland and coastal areas). EO also has the issue of only 'seeing' the top layers of vegetation when assessing the intertidal area specifically. Therefore, if one vegetation is covering another the satellite will only 'see' the topmost vegetation. This could cause under-prediction of seagrass, especially in situations where green algae or brown algae cover large areas of seagrass meadows. Likewise, while satellites such as Sentinel-2 have relatively small revisit times, the need for cloud free, low-tide imagery significantly decreases the number of useful images. Yet, here relatively high numbers of images were found for the sites selected. The site with the lowest number of images in a single year was 4 images in 2021 and 2022 for Santander Bay, while the greatest number of images in a single year was 24 in 2022 in Ria de Aveiro Coastal Lagoon. Over the whole time series Ria de Aveiro Coastal Lagoon had the greatest number of images ($N = 129$); while Santander Bay was the lowest 39 images were still utilised. This number of images covers areas far greater than an equivalent *in situ* method and costs significantly less, as they are effectively free to the end user.

5.3. Importance of trend analyses

As highly important providers of ecosystem services, global seagrass habitats are being increasingly assessed for health, loss, recovery and stability (Los Santos et al., 2019; Zoffoli et al., 2021). These assessments of status are frequently used as environmental monitoring tools assessed

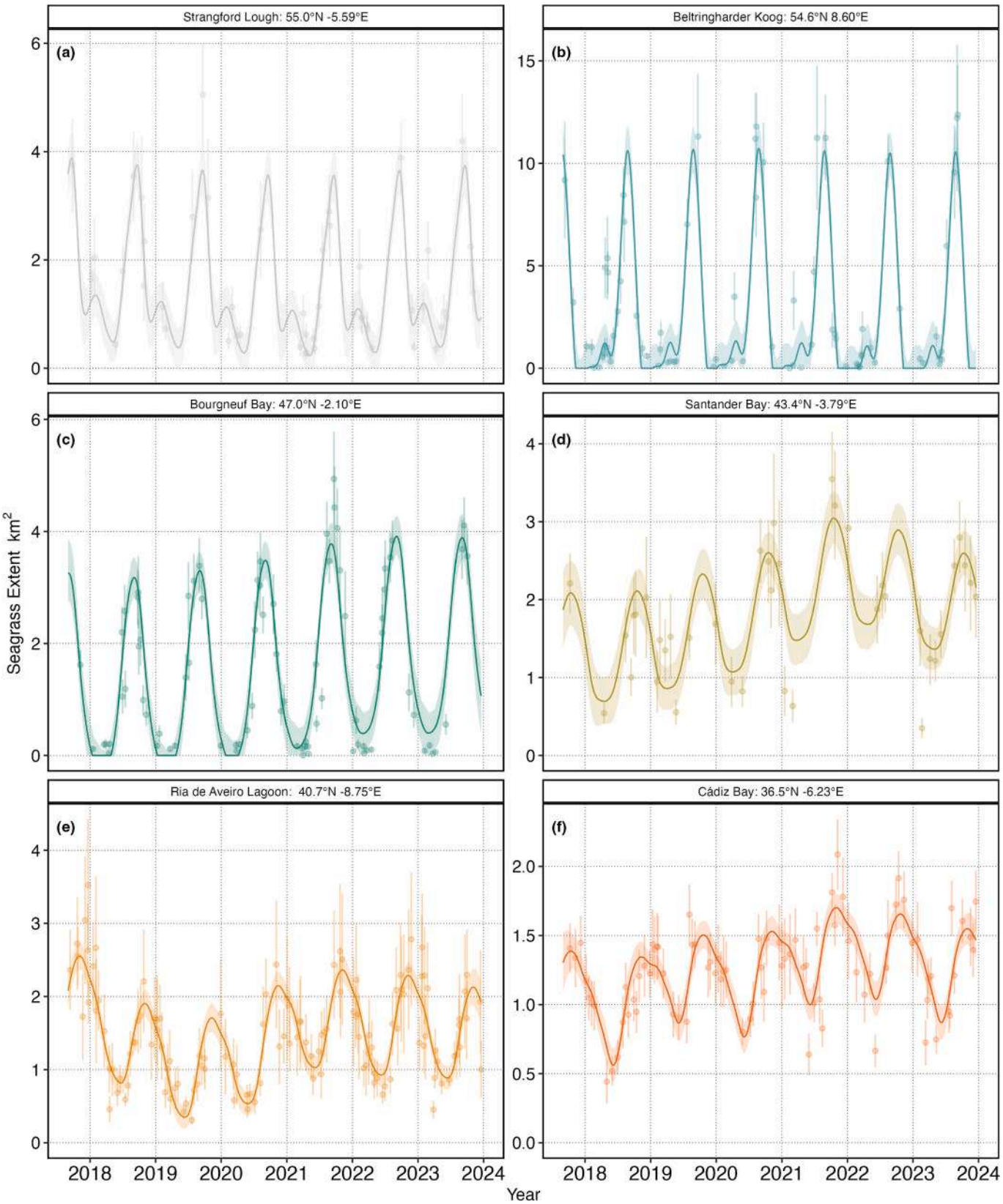

Fig. 6. Trend in intertidal seagrass extent (km^2) across six sites. Points with error bars show neural network estimated cumulative cover and average uncertainty per satellite image, while the dark line and shading show median and 89% confidence intervals across 2000 posterior predictive samples from a General Additive Model. Plot labels show the site and its latitude and longitude (in degrees) for a Strangford Lough, b Beltringharder Koog, c Bourgneuf Bay, d Santander Bay, e Ria de Aveiro Lagoon and f Cádiz Bay.

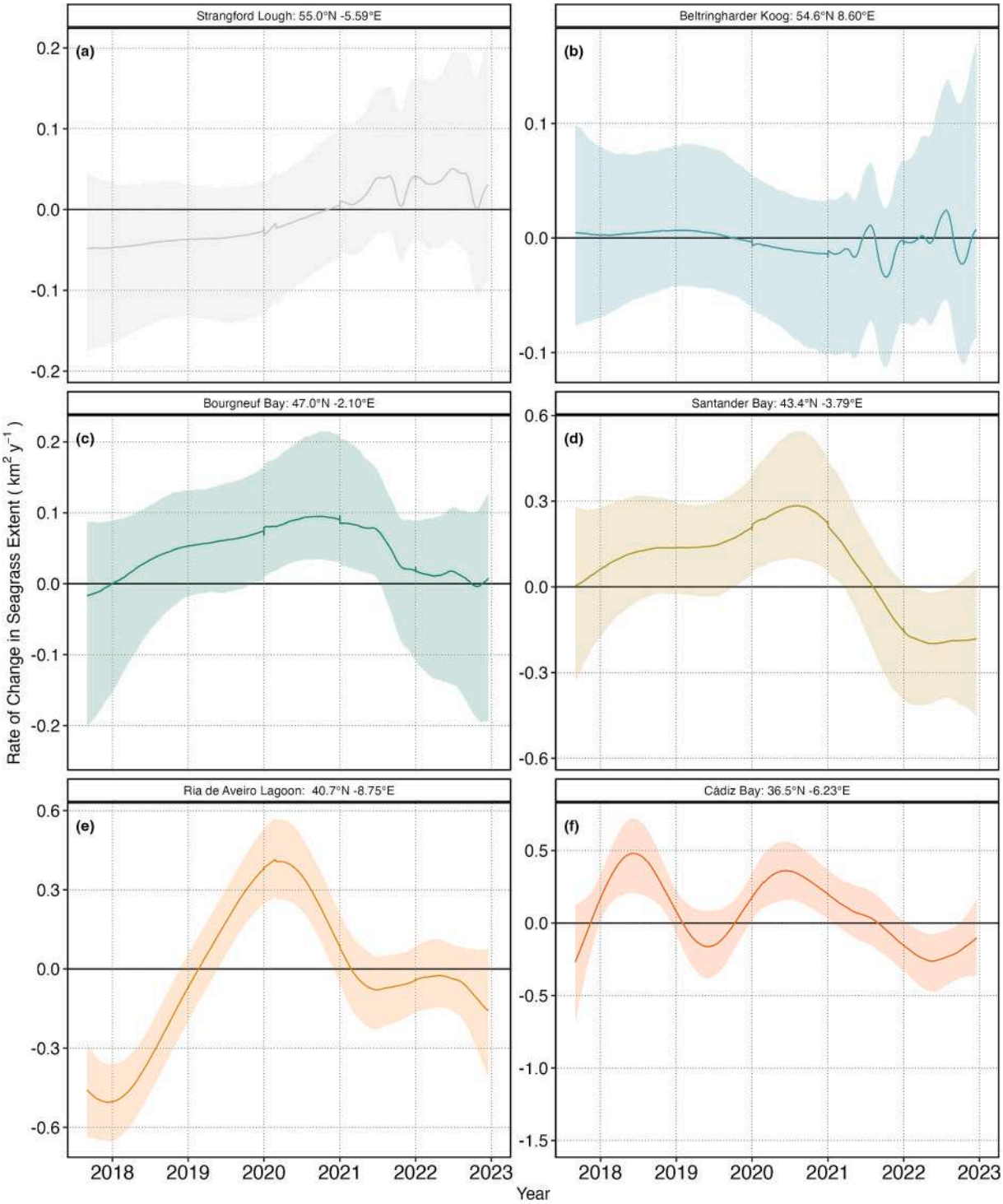

Fig. 7. Rate of change in cumulative seagrass extent in km^2 y $^{-1}$ derived from a General Additive Model. Lines show the median first derivative, while shaded areas show the 89% confidence intervals across 2000 posterior predictive samples from a General Additive Model. Plot labels show the site and its latitude and longitude (in degrees) for a Strangford Lough, b Beltringharder Koog, c Bourgneuf Bay, d Santander Bay, e Ria de Aveiro Lagoon and f Cádiz Bay.

at local, national or international scales to aid wider environmental and ecosystem management. One of the most well known examples of this is the EU Water Framework Directive (Foden and Brazier, 2007; WFD: Krause-Jensen et al., 2005), where seagrass is amongst other biological quality elements to assess the waters ecological status. However, to be able to assess the status of a wide-ranging habitat, such as seagrass, high levels of temporal and spatial data are needed (Papathanasopoulou et al., 2019; Zoffoli et al., 2021). Temporal span is arguably as important as temporal resolution; having an understanding of inter and intra-annual variation can aid more effective assessment of long-term trends and pave the way for more accurate future predictions (Dunic et al., 2021; Los Santos et al., 2019; McKenzie et al., 2020). The intertidal classifier developed in this work could help provide pan-European intertidal seagrass status, promoting the uptake of EO by future European Directives (Papathanasopoulou et al., 2019; Zoffoli et al., 2021). Climate change will affect all ecosystems on the planet in a myriad of

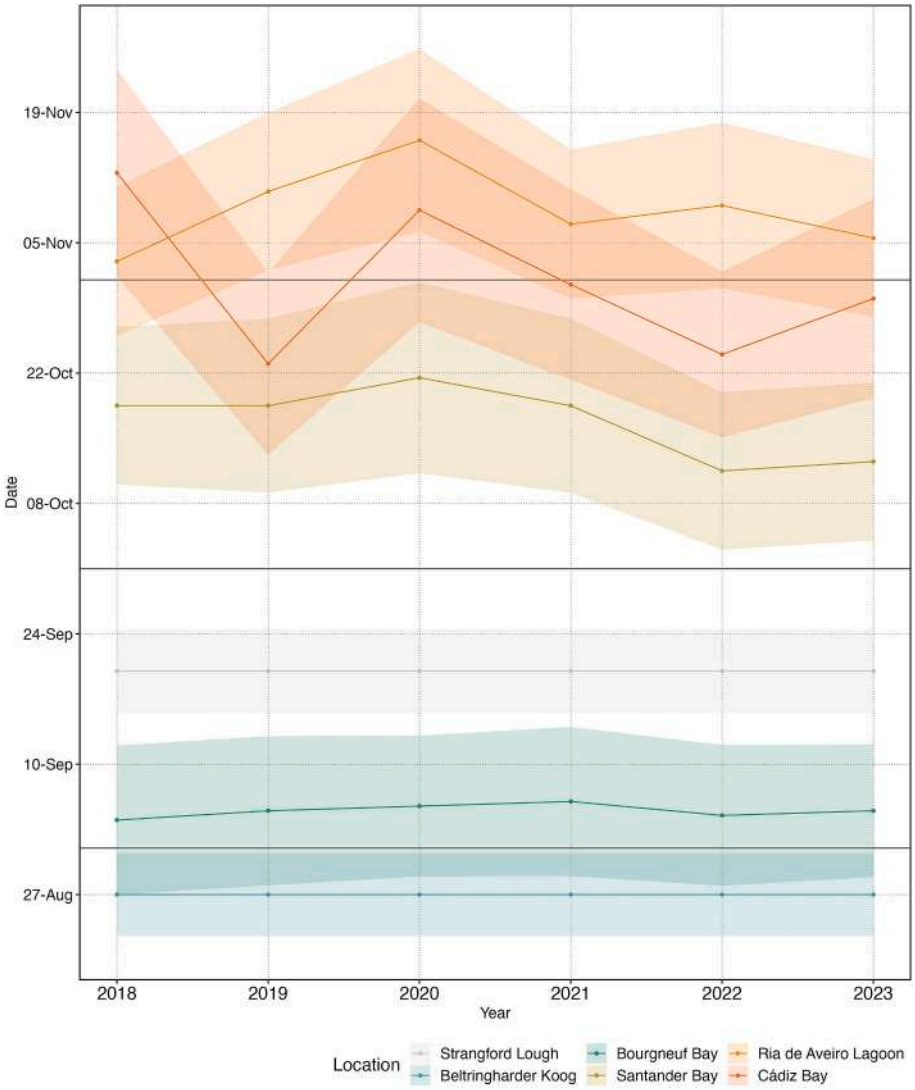

Fig. 8. Timing of maximum intertidal seagrass extent for each location from 2018 to 2023. Lines show median day of the year for modelled peak intertidal seagrass extent, shading shows 89% confidence intervals. Solid black horizontal lines show the first day of each month.

ways, many of which are currently unknown or poorly understood; thus, our understanding of how these essential habitats change over time is a prerequisite for effective prediction of future dynamics, especially in intertidal habitats directly threatened by sea level rise. Tools, such as the presented RS approach, are therefore highly important for building invaluable datasets to aid effective and reliable predictive models, but also to allow finer-scale assessments of current management strategies. However, to maximise the available data for these approaches, the outputs from models, such as ICE CREAMS, need to be either directly or indirectly comparable to historic and in situ collected data.

5.4. *Consistency of areal extent estimation*

While trends found elsewhere seem to concur with the current work, the difference in areas are not fully comparable, as different methods have been used across the literature. Here, Strangford Lough was found to maintain a consistent maximum area (~ 4.5 km^2) over the 7 years of Sentinel-2, yet the previous trends associated with the lough showed a decreasing trend of 15 to 9 km^2 from 1970 to 2003 (summarised by Los Santos et al., 2019). The values in the current survey are half those found by Los Santos et al. (2019), but a closer value was found in October 1991 of 6.2 km^2 (Portig et al., 1994), yet this method used belt transects of cores and extrapolated areas from cores to intertidal area. Likewise, there was strong corroboration to previous literature in Bourgneuf Bay where consistent increases have been quantified of 2 to 5.8 km^2 for 1991 to 2005 and 3 to 5.8 km^2 for 1985 to 2020 (Barillé et al., 2010; Zoffoli et al., 2021), which generally concurs with the estimated maximum extent of 4.9 km^2 found here, though these studies used a combination of different satellites and summed all pixels for ranges of specific NDVI values. Santander Bay was documented to increase from 0.2 to 0.6 km^2 but only within a total potential area of 1 km^2 from 1984 to 2015 (Calleja et al., 2017). In addition, in Ria de Aveiro Coastal Lagoon, intertidal seagrass mapped areas were estimated as ~2,3 km^2 in 2014 and ~ 1,2 km^2 in 2005 (Sousa et al., 2019), while the current study estimates a maximum extent of ~3.5 km^2 in 2017. All these estimates of extent and trends in intertidal seagrass extent utilised different sampling techniques with similarly different methods to quantify the total extent. These differences in methodology make exact comparisons impractical. Therefore, we suggest that a uniform approach to incorporating remote sensing assessments of intertidal seagrasses should be adopted. The summation of all cover (percentage) multiplied by their area, used here, could be used consistently across sensors and different spatial scales, but relies on the comparability of NDVI values across those sensors.

5.5. Utility for management

Total seagrass extent is generally one of the most common metrics of seagrass meadow health (Los Santos et al., 2019; Marbà et al., 2013; Romero et al., 2007). Yet, the method described here could be used to assess more finer scale, within-meadow fluctuations over time, thus allowing assessments of local trophic interactions (Chand and Bollard, 2022). For example, Bourgneuf Bay is mostly concentrated in one large meadow with very high density, whereas Strangford Lough is distributed in more disparate lower density patches (Fig. 5). The morphology and distribution of the intertidal seagrass beds may influence their reaction to impacts, with larger dense seagrass meadows providing higher survival rates, due to wave attenuation and resistance to sediment deposition (Inglis, 1999).

Likewise, location of the meadow in the intertidal area will be highly important, with greater vulnerability to sea-level rise if the vast majority of a meadow is closer to the lower edge of the intertidal area (Poppe and Rybczyk, 2022). Patterns of anthropogenic activity will also be localised to certain regions of the intertidal area, depending on the activity, and will thus influence different areas of the seagrass meadows (Turschwell et al., 2021). Fine scale dynamics of seagrass meadows, with potential to assess the recent past, would provide valuable insight to local managers in many different situations, with the ability to quantify local anthropogenic activities, such as aquaculture, channel dredging and boat anchoring (Barillé et al., 2010). Across the sites assessed here, the hydrological and bathymetric characteristics share a pattern of enclosed intertidal areas, yet they will vary in the level of exposure to wave action, nutrient flow, tidal regime and anthropogenic impacts. These differences will undoubtedly have a strong influence on the long-term trends in these meadows.

Furthermore, these data highlight the differences in phenological patterns, which will be equally important for management. The timing of seagrass maximum extent varied across sites, with generally a later maximum timing in the year the further south. This apparent latitudinally driven seasonal variation will be vital for the success of restoration efforts. The underlying mechanism that drives this change has not been assessed here, yet it is likely that a complex interaction of many abiotic factors may drive this change in phenology, such as, but not limited to, the air and sea temperature, the amount of incident solar radiation, the availability of nutrients, the tidal regime and the amount of suspended particulate matter at high tide.

6. Conclusions

Here, we demonstrate the utility of Sentinel-2 imagery alongside a neural network model to provide up-to-date high spatial resolution intertidal seagrass extent assessments. We found patterns of progressive increase across 7 years in seagrass meadow extent in sites that have previously been assessed for long term trends, while other sites showed no increase. These results provide an update to previous decadal analyses, as well as providing a process pipeline to create up-to-date monitoring data. The planned continuation of the Sentinel missions will allow continued almost real-time monitoring of these habitats. This process, and the data it provides, could be highly beneficial to both regional and international managers, with the ability to describe seagrass meadows at high spatial resolution, as well as high spatial scales. The importance of monitoring intertidal seagrasses at greater spatial and temporal resolution will allow for much more specific and rapid management measures.

CRediT authorship contribution statement

Bede Ffinian Rowe Davies: Writing – review & editing, Writing – original draft, Visualization, Validation, Software, Resources, Methodology, Investigation, Formal analysis, Data curation, Conceptualization. **Simon Oiry:** Writing – review & editing, Writing – original draft, Methodology, Data curation, Conceptualization. **Philippe Rosa:** Writing – review & editing, Methodology, Data curation. **Maria Laura Zoffoli:** Writing – review & editing, Methodology, Data curation. **Ana I. Sousa:** Writing – review & editing, Resources, Investigation. **Oliver R. Thomas:** Writing – review & editing, Resources, Investigation. **Dan A. Smale:** Writing – review & editing, Resources. **Melanie C. Austen:** Writing – review & editing, Resources. **Martin J. Attrill:** Writing – review & editing, Resources. **Alejandro Roman:** Writing – review & editing, Resources, Investigation. **Gabriel Navarro:** Writing – review & editing, Resources. **Anne-Laure Barillé:** Resources. **Nicolas Harin:** Resources. **Daniel Clewley:** Writing – review & editing, Resources, Methodology, Investigation. **Victor Martinez-Vicente:** Writing – review & editing, Project administration, Funding acquisition, Conceptualization. **Pierre Gernez:** Writing – review & editing, Writing – original draft, Supervision, Project administration, Methodology, Investigation, Funding acquisition, Conceptualization. **Laurent Barillé:** Writing – review & editing, Resources.

Declaration of competing interest

The authors declare that they have no known competing financial interests or personal relationships that could have appeared to influence the work reported in this paper.

Data availability

Data will be made available using a figshare link once the paper is published.

Acknowledgments

We would like to thank the three annonymous reviewers for their comments and corrections to improve the manuscript. This work was supported through the BiCOME (Biodiversity of the Coastal Ocean: Monitoring with Earth Observation) project funded by the European Space Agency under 'Earth Observation Science for Society' element of FutureEO-1 BIODIVERSITY+PRECURSORS call, contract No. 4000135756/21/I-EF. This work was also supported through the REWRITE (Rewilding European Shorelines and Beyond) project funded by the European Union under Grant Agreement 101081357. UAV data collection at Cádiz Bay was possible thanks to the SAT4ALGAE (PY20-00244) project by Junta de Andalucía, and A.R. is supported by grant FPU19/04557 funded by Ministry of Universities of the Spanish Government. Financial support from FCT- Fundação para a Ciência e Tecnologia (FCT/MCTES, Portugal) was also provided to A.I·S through the research contract CEECIND/00962/2017 (DOI: 10.54499/CEECIND/00962/2017/CP1459/CT0008) to the CESAM through the projects UIDB/50017/2020 + UIDP/50017/2020 + LA/P/0094/2020.

References

Ai, B., Wen, Z., Wang, Z., Wang, R., Su, D., Li, C., Yang, F., 2020. Convolutional neural network to retrieve water depth in marine shallow water area from remote sensing images. IEEE J. Select. Top. Appl. Earth Observ. Remote Sensing 13, 2888–2898.

Barillé, L., Robin, M., Harin, N., Bargain, A., Launeau, P., 2010. Increase in seagrass distribution at bourgneuf bay (France) detected by spatial remote sensing. Aquat. Bot. 92, 185–194. https://doi.org/10.1016/j.aquabot.2009.11.006.

Bürkner, P.-C., 2021. Bayesian item response modeling in R with brms and Stan. J. Stat. Softw. 100, 1–54. https://doi.org/10.18637/jss.v100.i05.

Calleja, F., Galván, C., Silió-Calzada, A., Juanes, J.A., Ondiviela, B., 2017. Long-term analysis of zostera noltei: a retrospective approach for understanding seagrasses' dynamics. Mar. Environ. Res. 130, 93–105.

Campbell, A.D., Fatoyinbo, L., Goldberg, L., Lagomasino, D., 2022. Global hotspots of salt marsh change and carbon emissions. Nature 612, 701–706.

Caparros-Santiago, J.A., Rodriguez-Galiano, V., Dash, J., 2021. Land surface phenology as indicator of global terrestrial ecosystem dynamics: a systematic review. ISPRS J. Photogramm. Remote Sens. 171, 330–347.

Carpenter, B., Gelman, A., Hoffman, M.D., Lee, D., Goodrich, B., Betancourt, M., Brubaker, M., Guo, J., Li, P., Riddell, A., 2017. Stan: a probabilistic programming language. J. Stat. Softw. 76.

Chand, S., Bollard, B., 2022. Detecting the spatial variability of seagrass meadows and their consequences on associated macrofauna benthic activity using novel drone technology. Remote Sens. 14 https://doi.org/10.3390/rs14010160.
Dai, Y., Yang, S., Zhao, D., Hu, C., Xu, W., Anderson, D.M., Li, Y., Song, X.-P., Boyce, D. G., Gibson, L., et al., 2023. Coastal phytoplankton blooms expand and intensify in the 21st century. Nature 615, 280–284.
Davies, B.F.R., Gernez, P., Geraud, A., Oiry, Simon, Rosa, P., Zoffoli, M.L., Barillé, L., 2023a. Multi-and hyperspectral classification of soft-bottom intertidal vegetation using a spectral library for coastal biodiversity remote sensing. Remote Sens. Environ. 290, 113554.
Davies, Bede Ffinian Rowe, Oiry, Simon, Rosa, Philippe, Zoffoli, Maria Laura, Sousa, Ana I., Thomas, Oliver R., Smale, Dan A., Austen, Melanie C., Biermann, Lauren, Attrill, Martin J., Roman, Alejandro, Navarro, Gabriel, Barillé, Anne-Laure, Harin, Nicolas, Clewley, Daniel, Martinez-Vicente, Victor, Gernez, Pierre, Barillé, Laurent, 2024. A sentinel watching over inter-tidal seagrass phenology across Western Europe and North Africa. Communications Earth & Environment 5 (1), 382.
Davies, B.F.R., Sousa, A., Figueira, R., Oiry, S., Gernez, P., Barillé, L., 2023b. Benthic intertidal vegetation from the tagus estuary and Aveiro lagoon. Version 1.6. Université de Nantes. In: Sampling Event Dataset. https://doi.org/10.15468/n4ak6x accessed via GBIF.org.
Devoy, R.J., 2008. Coastal vulnerability and the implications of sea-level rise for Ireland. J. Coast. Res. 24, 325–341.
Dierssen, H.M., Chlus, A., Russell, B., 2015. Hyperspectral discrimination of floating mats of seagrass wrack and the macroalgae sargassum in coastal waters of greater florida bay using airborne remote sensing. Remote Sens. Environ. 167, 247–258. https://doi.org/10.1016/j.rse.2015.01.027.
Douay, F., Verpoorter, C., Duong, G., Spilmont, N., Gevaert, F., 2022. New hyperspectral procedure to discriminate intertidal macroalgae. Remote Sens. 14, 346.
Dunic, J.C., Brown, C.J., Connolly, R.M., Turschwell, M.P., Côté, I.M., 2021. Long-term declines and recovery of meadow area across the world's seagrass bioregions. Glob. Chang. Biol. 27, 4096–4109.
Foden, J., Brazier, D.P., 2007. Angiosperms (seagrass) within the EU water framework directive: a UK perspective. Mar. Pollut. Bull. 55, 181–195. https://doi.org/10.1016/j.marpolbul.2006.08.021.
Gernez, P., Zoffoli, M.L., Lacour, T., Fariñas, T.H., Navarro, G., Caballero, I., Harmel, T., 2023. The many shades of red tides: Sentinel-2 optical types of highly-concentrated harmful algal blooms. Remote Sens. Environ. 287, 113486.
Guan, K., Wood, E.F., Medvigy, D., Kimball, J., Pan, M., Caylor, K.K., Sheffield, J., Xu, X., Jones, M.O., 2014. Terrestrial hydrological controls on land surface phenology of african savannas and woodlands. J. Geophys. Res. Biogeosci. 119, 1652–1669.
Hillebrand, H., Brey, T., Gutt, J., Hagen, W., Metfies, K., Meyer, B., Lewandowska, A., 2018. Climate change: warming impacts on marine biodiversity. In: Handbook on Marine Environment Protection: Science, Impacts and Sustainable Management, pp. 353–373.
Hoang, N.-D., Tran, X.-L., 2021. Remote sensing–based urban green space detection using marine predators algorithm optimized machine learning approach. Math. Probl. Eng. 2021, 1–22.
Howard, J., Gugger, S., 2020. Fastai: a layered API for deep learning. Information 11, 108. https://doi.org/10.3390/info11020108.
Inglis, G.J., 1999. Variation in the recruitment behaviour of seagrass seeds: implications for population dynamics and resource management. Pac. Conserv. Biol. 5, 251–259.
Jackson, E.L., Rees, S.E., Wilding, C., Attrill, M.J., 2015. Use of a seagrass residency index to apportion commercial fishery landing values and recreation fisheries expenditure to seagrass habitat service. Conserv. Biol. 29, 899–909.
Jia, M., Wang, Z., Mao, D., Ren, C., Song, K., Zhao, C., Wang, C., Xiao, X., Wang, Y., 2023. Mapping global distribution of mangrove forests at 10-m resolution. Sci. Bull. 68, 1306–1316.
Krause-Jensen, D., Greve, T.M., Nielsen, K., 2005. Eelgrass as a bioindicator under the european water framework directive. Water Resour. Manag. 19, 63–75.
Kutser, T., Hedley, J., Giardino, C., Roelfsema, C., Brando, V.E., 2020. Remote sensing of shallow waters–a 50 year retrospective and future directions. Remote Sens. Environ. 240, 111619.
Lamb, J.B., Van De Water, J.A., Bourne, D.G., Altier, C., Hein, M.Y., Fiorenza, E.A., Abu, N., Jompa, J., Harvell, C.D., 2017. Seagrass ecosystems reduce exposure to bacterial pathogens of humans, fishes, and invertebrates. Science 355, 731–733.
Lee, C.B., Martin, L., Traganos, D., Antat, S., Baez, S.K., Cupidon, A., Faure, A., Harlay, J., Morgan, M., Mortimer, J.A., et al., 2023. Mapping the national seagrass extent in Seychelles using PlanetScope NICFI data. Remote Sens. 15, 4500.
Li, A.S., Chirayath, V., Segal-Rozenhaimer, M., Torres-Perez, J.L., Bergh, J., 2020. NASA NeMO-net's convolutional neural network: mapping marine habitats with spectrally heterogeneous remote sensing imagery. IEEE J. Select. Top. Appl. Earth Observ. Remote Sensing 13, 5115–5133.
Lizcano-Sandoval, L., Anastasiou, C., Montes, E., Raulerson, G., Sherwood, E., Muller-Karger, F.E., 2022. Seagrass distribution, areal cover, and changes (1990–2021) in coastal waters off west-Central florida, USA. Estuar. Coast. Shelf Sci. 108134.
Los Santos, C.B., Krause-Jensen, D., Alcoverro, T., Marbà, N., Duarte, C.M., Van Katwijk, M.M., Pérez, M., Romero, J., Sánchez-Lizaso, J.L., Roca, G., et al., 2019. Recent trend reversal for declining european seagrass meadows. Nat. Commun. 10, 3356.
Losciale, R., Day, J.C., Rasheed, M.A., Heron, S.F., 2024. The vulnerability of world heritage seagrass habitats to climate change. Glob. Chang. Biol. 30, e17113.
Main-Knorn, M., Pflug, B., Louis, J., Debaecker, V., Müller-Wilm, U., Gascon, F., 2017. Sen2Cor for sentinel-2. In: Image and Signal Processing for reMote Sensing XXIII. SPIE, pp. 37–48.
Marbà, N., Krause-Jensen, D., Alcoverro, T., Birk, S., Pedersen, A., Neto, J.M., Orfanidis, S., Garmendia, J.M., Muxika, I., Borja, A., et al., 2013. Diversity of european seagrass indicators: patterns within and across regions. Hydrobiologia 704, 265–278.
Maxwell, A.E., Warner, T.A., Fang, F., 2018. Implementation of machine-learning classification in remote sensing: an applied review. Int. J. Remote Sens. 39, 2784–2817.
McKenzie, L.J., Nordlund, L.M., Jones, B.L., Cullen-Unsworth, L.C., Roelfsema, C., Unsworth, R.K.F., 2020. The global distribution of seagrass meadows. Environ. Res. Lett. 15.
Mora-Soto, A., Palacios, M., Macaya, E.C., Gómez, I., Huovinen, P., Pérez-Matus, A., Young, M., Golding, N., Toro, M., Yaqub, M., et al., 2020. A high-resolution global map of giant kelp (macrocystis pyrifera) forests and intertidal green algae (ulvophyceae) with sentinel-2 imagery. Remote Sens. 12, 694.
Murray, N.J., Phinn, S.R., DeWitt, M., Ferrari, R., Johnston, R., Lyons, M.B., Clinton, N., Thau, D., Fuller, R.A., 2019. The global distribution and trajectory of tidal flats. Nature 565, 222–225. https://doi.org/10.1038/s41586-018-0805-8.
Oiry, S., Barillé, L., 2021. Using sentinel-2 satellite imagery to develop microphytobenthos-based water quality indices in estuaries. Ecol. Indic. 121 https://doi.org/10.1016/j.ecolind.2020.107184.
Papathanasopoulou, E., Simis, S.G.H., Alikas, K., Ansper, A., Anttila, S., Jenni, A., Barillé, A.-L., Barillé, L., Brando, V., Bresciani, M., Bučas, M., Gernez, P., Giardino, C., Harin, N., Hommersom, A., Kangro, K., Kauppila, P., Koponen, S., Laanen, M., Neil, C., Papadakis, D., Peters, S., Poikane, S., Kathrin Poser, K., Pires, M. D., Riddick, C., Spyrakos, E., Tyler, A., Vaičiūtė, D., Warren, M., Zoffoli, M.L., 2019. Satellite-assisted monitoring of water quality to support the implementation of the water framework directive. EOMORES White Paper 28. https://doi.org/10.5281/zenodo.3463051.
Paul, M., Amos, C., 2011. Spatial and seasonal variation in wave attenuation over *Zostera noltii*. J. Geophys. Res. Oceans 116.
Phinn, S.R., Kovacs, E.M., Roelfsema, C.M., Canto, R.F., Collier, C.J., McKenzie, L., 2018. Assessing the potential for satellite image monitoring of seagrass thermal dynamics: for inter-and shallow sub-tidal seagrasses in the inshore great barrier reef world heritage area, Australia. Int. J. Digital Earth 11, 803–824.
Poppe, K.L., Rybczyk, J.M., 2022. Assessing the future of an intertidal seagrass meadow in response to sea level rise with a hybrid ecogeomorphic model of elevation change. Ecol. Model. 469, 109975.
Portig, A., Mathers, R., Montgomery, W., Govier, R., 1994. The distribution and utilisation of zostera species in strangford lough, Northern Ireland. Aquat. Bot. 47, 317–328.
R Core Team, 2023. R: A Language and Environment for Statistical Computing. R Foundation for Statistical Computing, Vienna, Austria.
Rankine, C., Sánchez-Azofeifa, G., Guzmán, J.A., Espirito-Santo, M., Sharp, I., 2017. Comparing MODIS and near-surface vegetation indexes for monitoring tropical dry forest phenology along a successional gradient using optical phenology towers. Environ. Res. Lett. 12, 105007.
Romero, J., Martinez-Crego, B., Alcoverro, T., Perez, M., 2007. A multivariate index based on the seagrass posidonia oceanica (POMI) to assess ecological status of coastal waters under the water framework directive (WFD). Mar. Pollut. Bull. 55, 196–204.
Shamsudeen, T.Y., 2020. Advances in remote sensing technology, machine learning and deep learning for marine oil spill detection, prediction and vulnerability assessment. Remote Sens. 12, 3416.
Sousa, A.I., Silva, J.F., Azevedo, A., Lillebø, A.I., 2019. Blue carbon stock in *Zostera noltei* meadows at ria de aveiro coastal lagoon (portugal) over a decade. Sci. Rep. 9, 14387.
Stan Development Team, 2018. RStan: The R Interface to Stan.
Su, H., Zhang, T., Lin, M., Lu, W., Yan, X.-H., 2021. Predicting subsurface thermohaline structure from remote sensing data based on long short-term memory neural networks. Remote Sens. Environ. 260, 112465.
Traganos, D., Reinartz, P., 2018. Mapping mediterranean seagrasses with sentinel-2 imagery. Mar. Pollut. Bull. 134, 197–209.
Traganos, D., Lee, C.B., Blume, A., Poursanidis, D., Čižmek, H., Deter, J., Mačić, V., Montefalcone, M., Pergent, G., Pergent-Martini, C., et al., 2022. Spatially explicit seagrass extent mapping across the entire mediterranean. Frontiers in marine. Science 9.
Turschwell, M.P., Connolly, R.M., Dunic, J.C., Sievers, M., Buelow, C.A., Pearson, R.M., Tulloch, V.J., Côté, I.M., Unsworth, R.K., Collier, C.J., et al., 2021. Anthropogenic pressures and life history predict trajectories of seagrass meadow extent at a global scale. Proc. Natl. Acad. Sci. 118, e2110802118.
Unsworth, R.K.F., McKenzie, L.J., Collier, C.J., Cullen-Unsworth, L.C., Duarte, C.M., Eklöf, J.S., Jarvis, J.C., Jones, B.L., Nordlund, L.M., 2019. Global challenges for seagrass conservation. Ambio 48, 801–815. https://doi.org/10.1007/s13280-018-1115-y.
Van Rossum, G., Drake, F.L., 2009. Python 3 Reference Manual. CreateSpace, Scotts Valley, CA.
Veettil, B.K., Ward, R.D., Lima, M.D.A.C., Stankovic, M., Hoai, P.N., Quang, N.X., 2020. Opportunities for seagrass research derived from remote sensing: a review of current methods. Ecol. Indic. 117, 106560.
Vilas, L.G., Spyrakos, E., Palenzuela, J.M.T., 2011. Neural network estimation of chlorophyll a from MERIS full resolution data for the coastal waters of galician rias (NW Spain). Remote Sens. Environ. 115, 524–535.
Waycott, M., Duarte, C.M., Carruthers, T.J., Orth, R.J., Dennison, W.C., Olyarnik, S., Calladine, A., Fourqurean, J.W., Heck Jr., K.L., Hughes, A.R., et al., 2009. Accelerating loss of seagrasses across the globe threatens coastal ecosystems. Proc. Natl. Acad. Sci. 106, 12377–12381.

Wood, S.N., 2017. Generalized Additive Models: An Introduction with r, 2nd ed. Hall/CRC, Chapman.

Zhong, L., Hu, L., Yu, L., Gong, P., Biging, G.S., 2016. Automated mapping of soybean and corn using phenology. ISPRS J. Photogramm. Remote Sens. 119, 151–164.

Zoffoli, M.L., Gernez, P., Rosa, P., Le Bris, A., Brando, V.E., Barillé, A.L., Harin, N., Peters, S., Poser, K., Spaias, L., Peralta, G., Barillé, L., 2020. Sentinel-2 remote sensing of *Zostera noltei*-dominated intertidal seagrass meadows. Remote Sens. Environ. 251, 112020 https://doi.org/10.1016/j.rse.2020.112020.

Zoffoli, M.L., Gernez, P., Godet, L., Peters, S., Oiry, S., Barillé, L., 2021. Decadal increase in the ecological status of a North-Atlantic intertidal seagrass meadow observed with multi-mission satellite time-series. Ecol. Indic. 130 https://doi.org/10.1016/j.ecolind.2021.108033.

Zoffoli, M.L., Gernez, P., Oiry, S., Godet, L., Dalloyau, S., Davies, B.F.R., Barillé, L., 2022. Remote sensing in seagrass ecology: coupled dynamics between migratory herbivorous birds and intertidal meadows observed by satellite during four decades. Remote Sens. Ecol. Conserv. 9 (3), 420–433.